International Journal of Thermal Sciences 147 (2020) 106133

Contents lists available at ScienceDirect

International Journal of Thermal Sciences

journal homepage: http://www.elsevier.com/locate/ijts

Optimization design of slotted fins based on exergy destruction minimization coupled with optimization algorithm

Shicheng Wang [b,1], Biao Xiao [a,1], Ya Ge [b], Lin He [a], Xiang Li [a], Wei Liu [b], Zhichun Liu [b,*]

[a] State Key Laboratory of Air-conditioning Equipment and System Energy Conservation, GREE Electric Appliances Inc., Zhuhai 519070, China
[b] School of Energy and Power Engineering, Huazhong University of Science and Technology, Wuhan, 430074, China

ARTICLE INFO

Keywords:
Slotted fin
Optimization
Exergy destruction minimization
Genetic algorithm
Neural network

ABSTRACT

In this paper, the influence of the slot parameters of the slotted fins on the flow and heat transfer performance and the exergy destruction are studied by numerical simulation, and the optimal parameters corresponding to the best overall performance and the minimum exergy destruction are obtained by the method of CFD coupled with optimization algorithm, respectively. In current work, the slot length and width are taken as parameters (slot length 1.2–2.1 mm, slot width 0.1–1.0 mm), 100 different cases are studied under the same boundary conditions, and the results are analyzed and optimized by the neural network and genetic algorithm. The overall performance is taken as the evaluation of the heat transfer performance and the power consumption, while exergy destruction caused by heat transfer and fluid flow are taken as the estimate of the loss of available energy and mechanical work. The results show that the overall performance is best when the slot length and width are 1.38 mm and 0.27 mm respectively, and the overall performance is 13.1% higher than that of flat fin. While the exergy destruction caused by heat transfer and fluid flow are minimized synergistically when the slot length and width are 1.37 mm and 0.12 mm, and the irreversible loss caused by heat transfer is reduced by 19.13%, at the cost of an increase of 40.6% in the irreversible loss caused by fluid flow. The difference between the parameters corresponding to best overall performance and exergy destruction minimization means the irreversible loss of heat transfer and fluid flow process is not minimum when the overall performance is best, and indicates the exergy destruction minimization can be a principle to evaluate the heat transfer and flow process. The result in this paper is of great significant to the energy utilization and the improvement of the thermal quality in waste heat recovery.

1. Introduction

Finned tube heat exchangers are widely used in power, chemical, petrochemical and refrigeration engineering. It is meaningful to improve the heat transfer performance of the finned tube heat exchangers to save the energy consumption and the economic costs. The thermal resistance of the heat transfer process in the fin tube bundles consists of three parts: convective heat transfer resistance on the air side, conductive thermal resistance of the metal wall and the convective heat transfer resistance on the liquid side inner the tube [1,2]. The thermal resistance on the air side is the largest because of the low thermal conductivity of the air, so the key to improving the performance of the heat exchangers is to enhance the heat transfer and fluid flow performance in the air side [3,4]. Compared to the flat fin surface, the use of enhanced fin surface can greatly improve the heat transfer performance and it is the most effectively way to reduce the thermal resistance in the air side [5,6]. There are already many enhanced surfaces developed, such as slotted fin, louver fin, wavy fin and [7] vortex generators [8]. And the enhanced surfaces can effectively increase the surface area, disturb the fluid flow [9] and prevent the development of boundary layer, at the same time, it leads to greater pressure loss. Among all of the enhanced surfaces, the slotted fins are more attractive to many researchers because of their simple geometric structure, good heat transfer enhancement with relatively low pressure drop [10,11]. The performance of slotted fin tube heat exchangers is related to many parameters [12], and the geometric parameters independent of the fin surface including tube pitch [13,14], fin thickness and fin pitch [15] and son on. However, when the space of the heat exchanger is fixed, it is very

* Corresponding author.
E-mail address: zcliu@hust.edu.cn (Z. Liu).
[1] Biao Xiao and Shicheng Wang contributed equally to this work.

https://doi.org/10.1016/j.ijthermalsci.2019.106133
Received 20 March 2019; Received in revised form 16 September 2019; Accepted 7 October 2019
Available online 14 October 2019
1290-0729/© 2019 Elsevier Masson SAS. All rights reserved.

difficult to further improve the performance by optimizing these parameters. So many researchers have studied the effects of slot parameters of the slotted fins on the performance improvement of the heat exchangers. The study shows that the performance of continuous slotted fins is higher than that of the alternating slotted fins [16]. Different types of slots can generate different types of vortexes and thus have different performance [17], because the intensity of the secondary flow on the fin surface determines the flow heat transfer characteristics of the slotted fin tube heat exchangers [18]. From the perspective of the nature of heat transfer enhancement, the filed synergy principle [19–21] are adopted to analyze the changes of the filed synergy angle, and the analysis results shows that the influence of various parameters on the overall performance can be well described and explained by the synergy principle [22–24].

However, the studies mentioned above mainly focus on increasing the heat transfer, which is based on the first law of thermodynamics, and only the temperature or the heat flux are considered. From the perspective of the second law of thermodynamics, not only the quantity in the heat transfer, but also the quality should be considered. Therefore, for the heat transfer and fluid flow in the finned tube heat exchangers, the heat transfer should be enhanced and the irreversible loss of the heat transfer process as well as the power consumption should be reduced. And the new alternative criterions based on the second thermodynamics are proposed to guide the optimization of flow and heat transfer, such as entropy generation minimization [25,26], entransy [27], available potential [28] and the expression of local exergy destruction derived from the equation of available potential. Different from entransy or entransy dissipation, the local exergy destruction is not only suitable for evaluating the irreversibility of heat transfer process, but also for the fluid flow, and the exergy destruction caused by fluid flow are proposed [28]. The exergy destruction caused by heat transfer represents the loss of the available energy, while the exergy destruction caused by flow fluid represents the power consumption and it fully represents the loss of mechanical work. The research demonstrated the approach of exergy destruction minimization is an effective way to optimize the convective heat transfer and it differs from the approach which taking the overall performance as the objective [29]. Moreover, the exergy efficiency is an effective evaluation criterion for convective heat transfer [30]. In order to develop a new method to guide the heat transfer optimization, it is necessary to analyze the distribution of the temperature in the whole filed, which is of great significance in practical engineering.

Due to the complexity of the geometry of the slotted fins, it is difficult to adopt the traditional optimization design method to find the optimal geometric parameter configuration, which is mainly based on empirical chosen and the results of predecessors [31] and could only find the local optimal solution. Therefore, during the design of the finned tube heat exchanger, it is necessary to find the global optimal solution by the optimization algorithm [32,33]. Recently, some studies have applied genetic algorithm (GA) to heat transfer optimization of fined tube heat exchangers [34–36], and found that the GA can get the global optimal solutions within a limited range [37–40]. While the artificial neural network (ANN) can make a good prediction of the unknown results based on the existing results, which greatly saves the computational costs [41–43]. And the key to obtaining a suitable ANN is to get the appropriate activation function and training function by training the data set.

As mentioned above, in the published literature, they mainly studied the slotted fin geometry parameters based on the first law of thermodynamics, and little research studied the effect of the slot size on the performance of slotted fins. So, in this paper, both from the perspective of the first law of thermodynamics and second law of thermodynamics, the effects of the slot length and width on the fin performance are studied. In order to achieve the best performance of the heat exchangers, the overall performance and exergy destruction are taken as optimization objective respectively, and the optimization algorithm is used to find the optimal slot parameters.

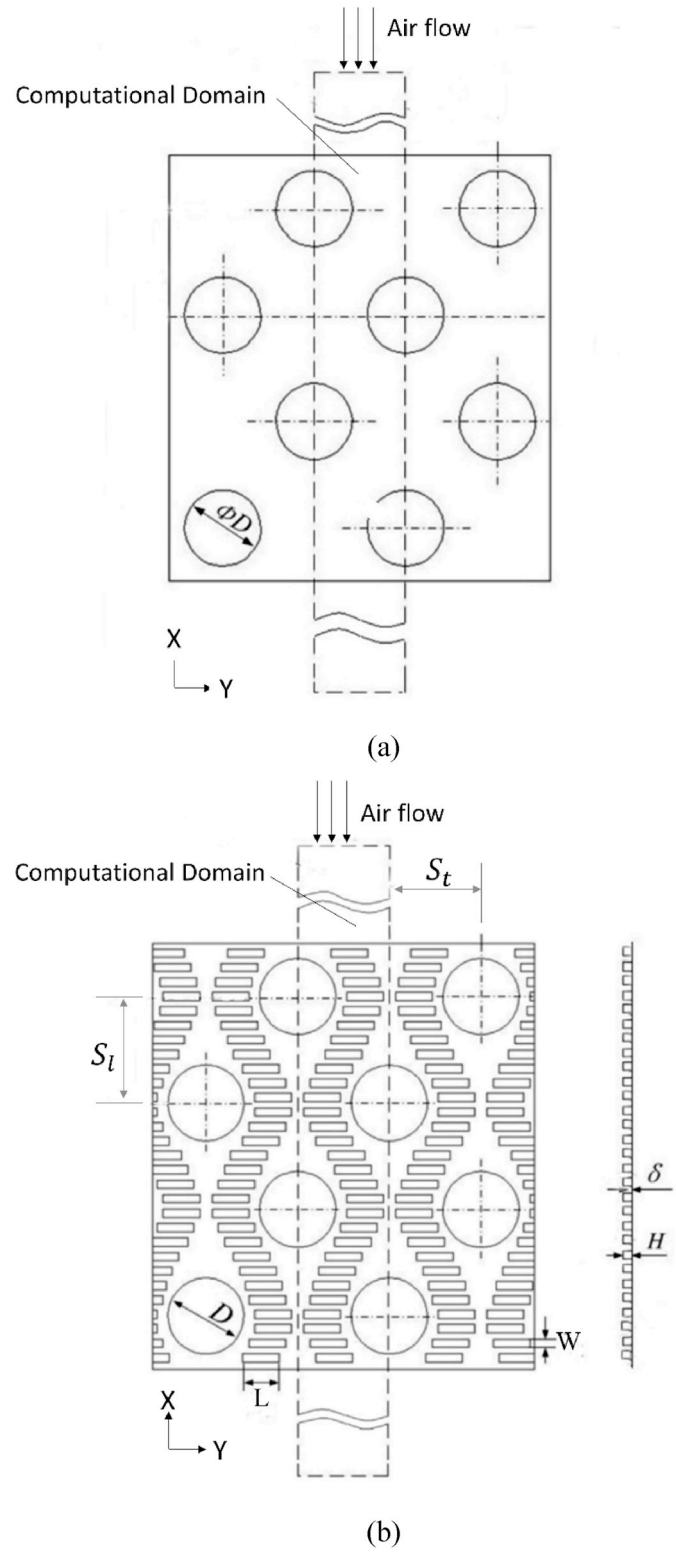

Fig. 1. Physical model of the fin tube bundles (a) flat fin (b) slotted fin.

2. Numerical simulation

2.1. Physical model

The flat and slotted fin tube bundles are shown in Fig. 1, and the four tubes are arranged staggered along the flow direction. Except some slotted blocks on the slotted fin surface, which are continuously

Table 1
Detailed geometric parameters of the slotted fins and flat fins.

Parameters	Value	
	slotted fin	flat fin
Fin thickness (δ/mm)	0.3	0.3
Fin pitch (mm)	2	2
Slot pitch (mm)	1	1
Diameter of tube (D/mm)	8	8
Transverse tube pitch (S_t/mm)	6.6	6.6
Longitudinal tube pitch (S_l/mm)	21	21
Length of the fin (L_{fin} mm)	80	80
Length of the inlet section (mm)	80	80
Length of the outlet section (mm)	260	80
Material	Aluminum	Aluminum
Length of slots (L/mm)	1.2–2.1	/
Width of slots (W/mm)	0.1–1.0	/
Height of strips (H/mm)	2.25	/

configured, as shown in Fig. 1(b), the parameters of slotted fin surface are the same as that of flat fin, such as the fin thickness, the fin pitch and tube pitch and so on. The detailed parameters of the fin tube bundles are listed in Table 1.

The regions enclosed by the dotted line shown in Fig. 1 is selected as computational domain, the computational domains of flat and slotted fins as well as the boundary conditions are shown in Fig. 2. The central part of the computational domain along the Z direction is the solid fin domain, while the upper and lower domain are the gas domains that surround the solid fins, which is clearly shown in Fig. 2(a). The upper and lower surfaces are set as periodic boundaries; while the left and right surfaces are set as symmetry boundaries. The velocity of gas at the inlet is constant at 5.72 m/s, the temperature of the gas is constant at 293 K. Since the finned tube heat exchanger is designed to meet the heat dissipation requirements under fixed heat loads, so the heat flux of the wall is considered as constant and the heat flux is 19436 W/m^2. To avoid the influence of the backflow at the outlet and to ensure the uniformity of the velocity at the inlet, the outlet extends 260 mm downstream and the inlet extends 80 mm upstream, which called as the outlet and inlet domain, shown in Fig. 2, so the pressure outlet is specified at the outlet. The central domain where solid fins exist is the core computational domain.

2.2. Governing equations and parameter definitions

Numerical simulation approach is used to study the three-dimensional steady, turbulent flow and heat transfer characteristics on the fin surfaces, and the coupling between fluid and solid is considered. Due to the temperature difference is not significant in the whole filed, the air is considered as incompressible fluid with constant physical properties. The governing equations to be solved include continuity, momentum and energy equations, they are given in the following forms: continuity equation:

$$\frac{\partial(\rho u_i)}{\partial x_i}=0 \tag{1}$$

and momentum equations:

$$\frac{\partial}{\partial x_i}(\rho u_i u_k)=\frac{\partial}{\partial x_i}\left(\mu\frac{\partial u_k}{\partial x_i}\right)-\frac{\partial p}{\partial x_k} \tag{2}$$

and the energy equation:

$$\frac{\partial}{\partial x_i}(\rho u_i T)=\frac{\partial}{\partial x_i}\left(\frac{\lambda}{C_p}\frac{\partial T}{\partial x_i}\right) \tag{3}$$

where λ is thermal conductivity of the air, and C_p is the specific heat capacity of the air.

The effect of turbulence on the fluid flow is included by applying the k − ε model. As for the physical properties of the air, firstly the physical properties are obtained at the inlet temperature T_{in} and the outlet temperature T_{out} is known after the numerical simulation, and then the physical properties are obtained at the mean temperature $(T_{in}+T_{out})/2$, then the second simulation is carried out and a new T_{out1} is obtained. Due to the difference between the air physical properties obtained at the mean temperature $(T_{in}+T_{out})/2$ and $(T_{in}+T_{out1})/2$ is negligible, so the physical properties of air are obtained at the mean temperature $(T_{in}+T_{out})/2$ in the following simulation, which is 329.5 °C. the T_{in} and T_{out} are the temperature of air at inlet and outlet, respectively. The coupling of pressure and velocity is solved by SIMPLE algorithm, and the convergence criteria of the continuity, momentum and energy are 10^{-4}, 10^{-6} and 10^{-8}, respectively.

The distributions of temperature and pressure throughout the flow field is non-uniform, and the temperature at each point on the surface is different, so the mass weighted average method is adopted to obtain the average temperature and pressure at the inlet and outlet. The average temperature and pressure of the gas are defined as follows:

$$\overline{T}=\frac{\int \rho u\cdot T\cdot dA}{\int \rho u\cdot dA} \tag{4.1}$$

$$\overline{p}=\frac{\int \rho u\cdot p\cdot dA}{\int \rho u\cdot dA} \tag{4.2}$$

In order to better describe the results, some dimensionless parameters for evaluating the performance of the finned tube bundles are defined. The Reynolds number and friction factor are defined as follows:

$$\mathrm{Re}=\frac{\rho u_{\mathrm{Amin}} D_h}{\mu} \tag{5}$$

$$f=\frac{\Delta p}{0.5\rho u_{\mathrm{Amin}}^2} \tag{6}$$

The u_{Amin} is the velocity at the minimum flow area, Δp is the pressure drop between inlet and outlet, $\Delta p = p_{in} - p_{out}$.

The Nusselt number is defined as:

$$Nu=\frac{hD_h}{\lambda} \tag{7}$$

$$D_h=\frac{4A_c L_{fin}}{A_0} \tag{8}$$

where h is the average heat transfer coefficient, defined as:

$$h=\frac{Q}{\Delta T\cdot A} \tag{9}$$

Q is the total heat flux rate, calculated by the expression:

$$Q=\dot{m}C_p(T_{in}-T_{out}) \tag{9.1}$$

and ΔT is the logarithmic mean temperature difference, calculated by the expression:

$$\Delta T=\frac{(T_w-T_{in})-(T_w-T_{out})}{\ln((T_w-T_{in})/(T_w-T_{out}))} \tag{9.2}$$

In order to better compare the overall performance between finned tube bundles with different parameters, a dimensionless evaluation index j_C is defined, and the expression of j_C is given below:

$$j_C=\frac{Nu/Nu_0}{(f/f_0)^{1/3}} \tag{10}$$

where Nu_0 and f_0 is the Nusselt number and friction factor of the flat fin, the larger j_C is, the better the overall performance of the finned tube bundles is.

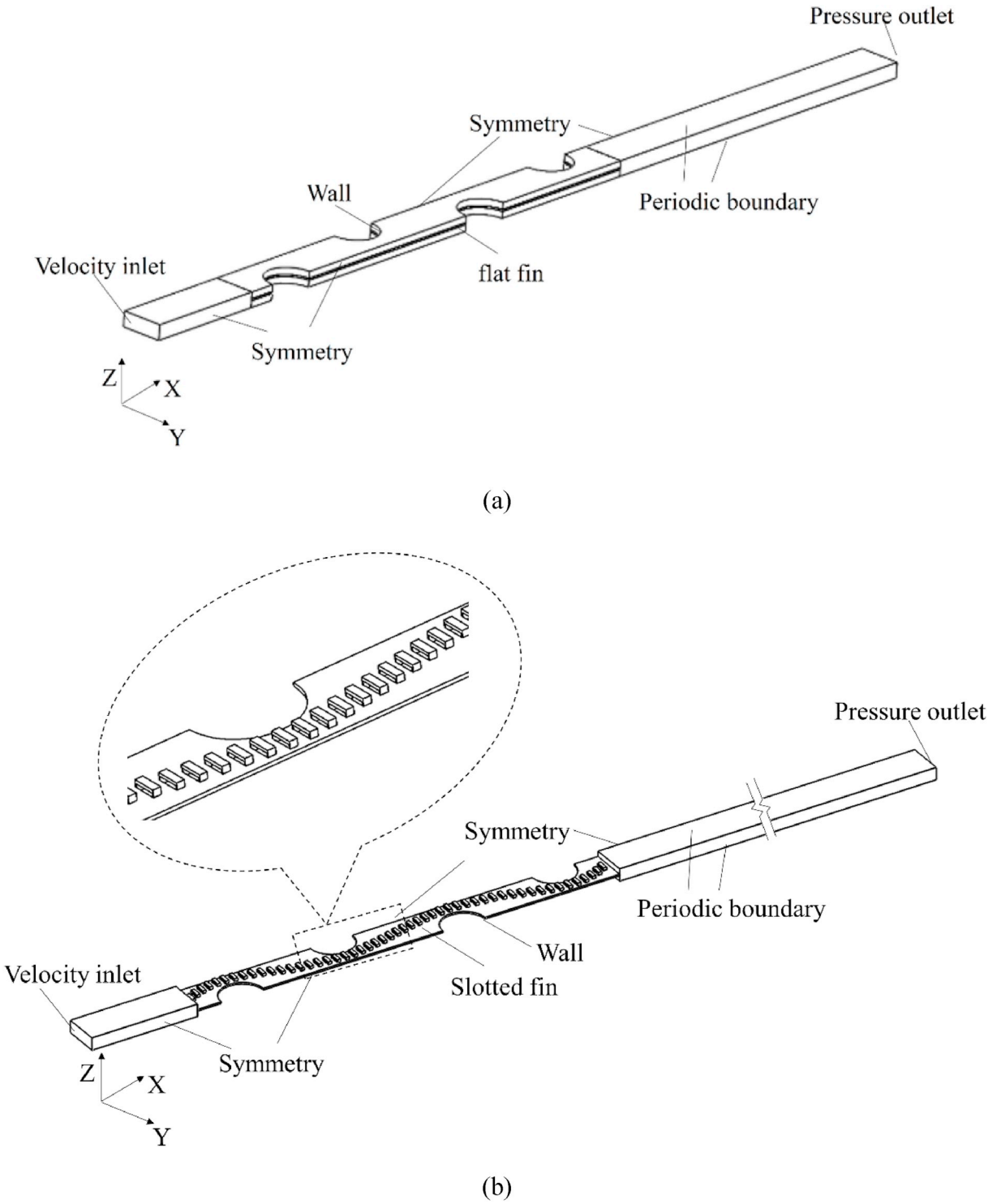

Fig. 2. Computational domain and boundary conditions (a) flat fin (b) slotted fin.

As mentioned above, the irreversibility must be taken into account, so to quantitatively evaluate the irreversibility of the flow and heat transfer process, the local exergy destruction caused by heat transfer are introduced below [28]:

$$i_o = T_0 \frac{\lambda(\nabla T)^2}{T^2} \tag{11}$$

where T_0 is the ambient temperature, and the total exergy destruction in the flow region is obtained by integration $I_0 = \iiint i_0 dV$. Meanwhile, the local exergy destruction caused by fluid flow [28]:

$$i_1 = u.\nabla p \tag{12}$$

the total exergy destruction caused by fluid flow in the flow region is obtained by integration $I_1 = \iiint i_1 dV$. The exergy destruction caused by fluid flow completely represents the loss of mechanical work, and the higher it is, the larger the power consumption is, so reducing the loss can help to reduce the flow power consumption. However, I_1 and I_0 are not independent, and the decrease of I_0 leads to the increase of I_1. So this

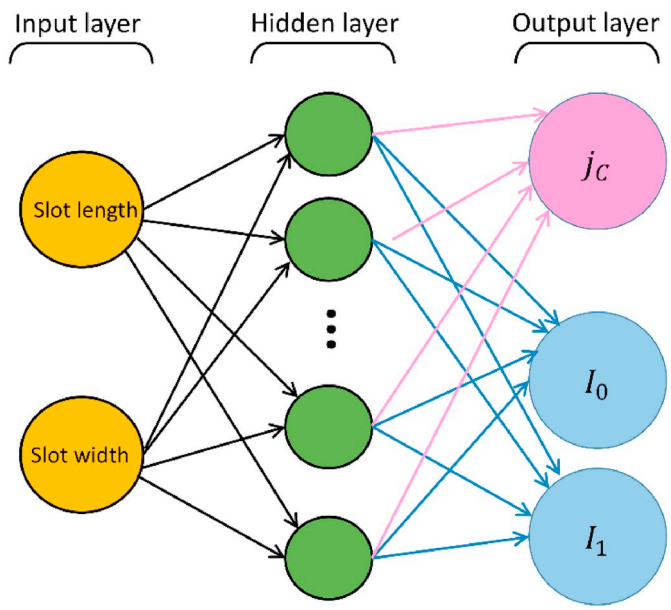

Fig. 3. The structure of neural network.

study aims to optimize the geometric parameters of the fin surface so that the two exergy destruction can achieve synergistic minimization.

2.3. Design of optimization algorithm model

There are 100 sets of results in this paper, and the results are processed by the optimization algorithm. Firstly, the artificial neural network (ANN) is applied to train the results [44], the structure of the ANN is shown in Fig. 3, there are two inputs, and one or two outputs according to the different objectives. Two kinds of evaluation criteria of the optimization design are considered: one is the overall performance based on the first law of thermodynamics and there is only one output j_C; the other is the exergy destruction minimization based on the second law of thermodynamics and there are two outputs, namely, exergy destruction caused by fluid flow I_1 and heat transfer I_0. With the well-trained ANN, the output results beyond the 100 sets of parameters can be well predicted [45], without calling the CFD software, and it is obviously that this approach saves much time and costs. By adjusting the training parameters of the neural network, the precision of the outputs can be precisely controlled [45], for the training data, the most deviation between the existing results and the predicting results is 6%, so the well-trained ANN is reliable.

The genetic algorithm (GA) is used to find the optimal solutions. The well-trained ANN is taken as the database of the GA, and the geometric parameters of the GA fitness function are entered to the database and then the results are retrieved from the database, the coupling between the ANN and the GA is shown in Fig. 4. The GA is an algorithm that simulates the biological evaluation to find the optimal solutions [46] after selection, crossover and mutation, namely, eliminate inferior individuals and produce next generation populations. The initial individuals are generated from the search space, and the fitness value are evaluated and assigned by the fitness function, and the fitness function is based on the objectives, the individuals with high fitness value have the chance to survive to the next generation. In this work, the search space of the slot width is ranging from 0.1 mm to 1.0 mm; and the slot length is ranging from 1.0 mm to 2.5 mm. After the optimization, the optimal overall performance and the minimum exergy destruction in the search space is obtained.

The overall performance and the exergy destruction are optimized separately as two different objectives, so two sets of neural network structures are used, as shown in Fig. 3. The input parameters of the two structures are both the slot length and the slot width, and for both of the structures, there are single hidden layers, single input layers and single output layers. For the optimization of single objective j_C, the TRAINLM function is adopted as the training function, and TANSIG function is adopted as the activation function, and the initial population of the genetic algorithm is taken as 50, the generations of evolution are 50, the convergence criterion is 10^{-6}. For the optimization of objectives I_0 and I_1, the TRAINBR function is adopted as the training function and the TANSIG function is adopted as the activation function, the initial population of the GA is 70, the evaluation generations are 1000, the

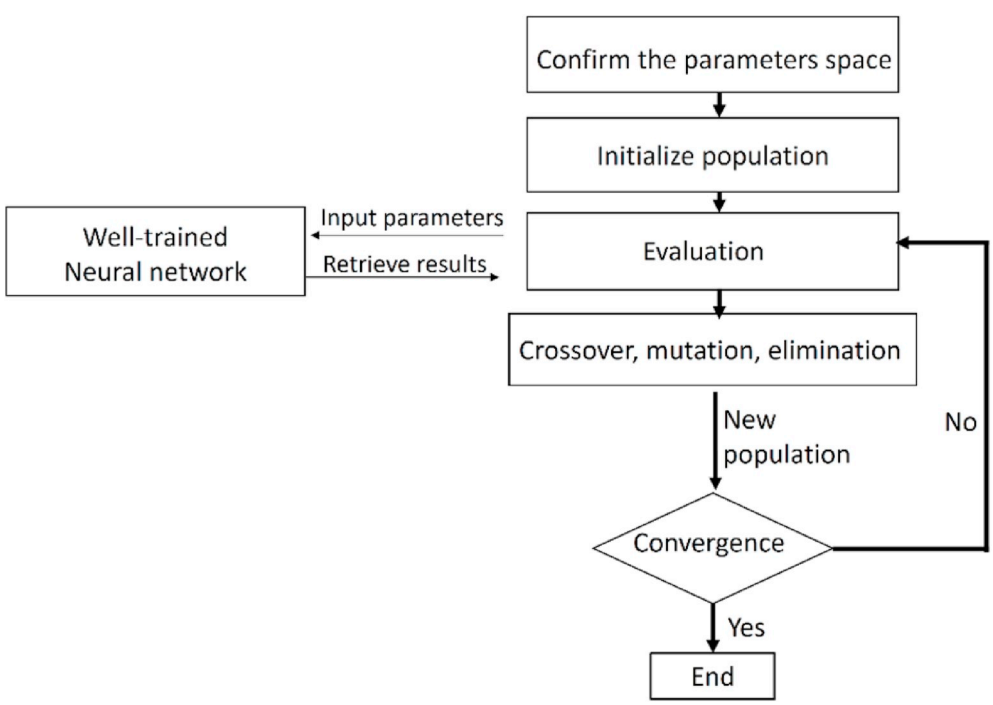

Fig. 4. Flow chart of genetic algorithm combined with neural network.

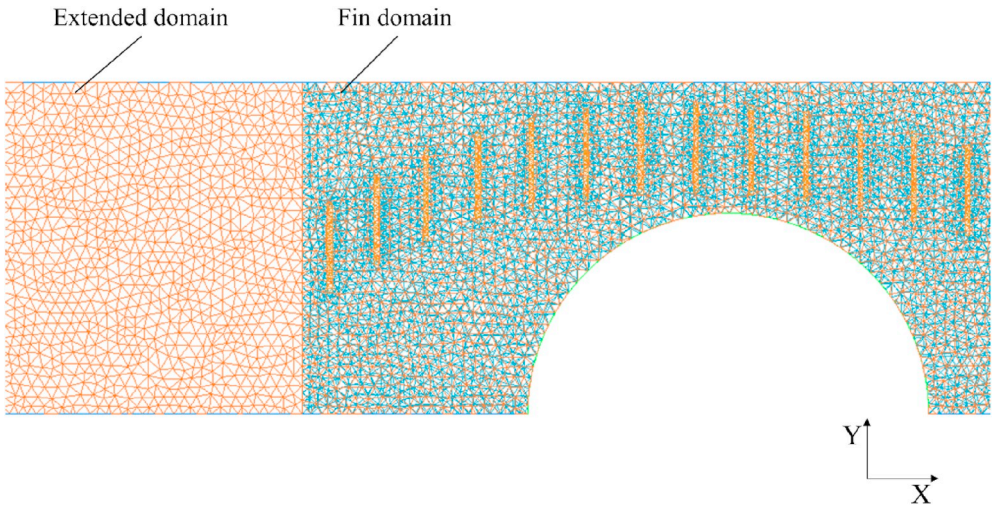

Fig. 5. Grid details near the extended and fin domains.

Table 2
Grid independence of heat transfer coefficient.

Grids number	1701926	2279893	2901137	3806333
Heat transfer coefficient (W/m^2·K)	37.6	38.3	38.5	38.6
Deviation (%)	2.00	0.55	0.235	/
Deltap	1050.52	1066.42	1099.191	1094.37
Deviation (%)	4.01	2.55	−0.44	/

convergence criterion is 10^{-6}.

2.4. Grid independence and model validation

In order to avoid the impact of the grid numbers on the results, it is necessary to verify the independence of the grid numbers. The unstructured grids are used to generate the computational grids because the geometry of the slotted fin is complicated. Generally, the grids near the wall is refined, especially for the wall near the slot where the swirling flow exists, and the grids in the inlet and outlet sections are coarse to save the time and cost, the grid details neat the extended and fin domains are shown in Fig. 5. The slotted fin with the slot length 2.1 mm and the width 1.0 mm is selected for the grid independence study, and the results are shown in Table 2. The results of the grids number 3806333 are selected as the reference, and it can be found that the deviation of the heat transfer coefficient of the grid number 2901137 and the grid number 3806333 is 0.235%, while the deviation of the Δp is −0.44%. Therefore, the grid number 2901137 is used as the final computational grid number, and the maximum element size is 0.45 mm.

In order to verify the reliability of the numerical model, it is necessary to compare the computational results with the experimental data. The numerical simulation is carried out on the flat fins, the results are compared with experimental data [47] and simulation data [48]. As shown in Fig. 6, the results show well agreement of the Nusselt number *Nu* and the pressure drop Δp with the experimental data and the simulation data. Although the highest deviation of the *Nu* is 8.31% when the *Re* is 2399, the highest deviation of pressure Δp is 13.88% when the *Re* is 2399, the allowable deviation of the correlation is within 15%, so it is reasonable to believe the numerical model is reliable, and it is also acceptable in engineering application. Moreover, the deviation is highest when the *Re* is 2399, this is because when *Re* is small, the flow state is close to the transition zone from laminar flow to turbulent flow, the turbulence model is not suitable for this zone, so the deviation is large. But in the following studies, the *Re* is far away from the transition zone.

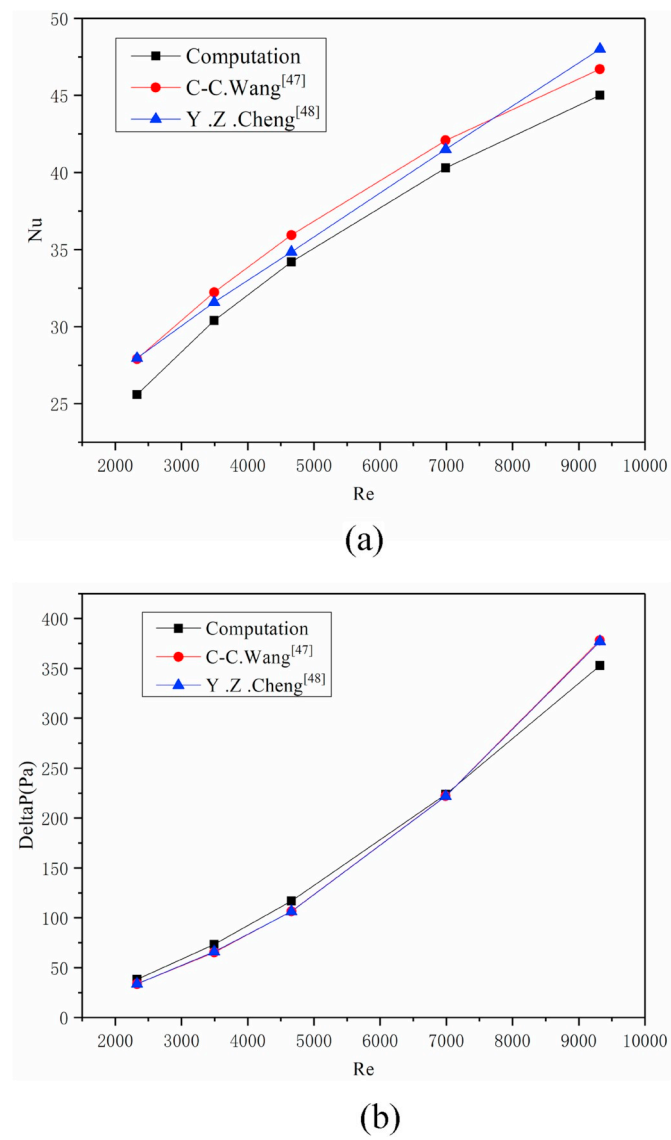

Fig. 6. Model validation of the numerical results (a) comparison of the *Nu* (b) comparison of the pressure drop Δp.

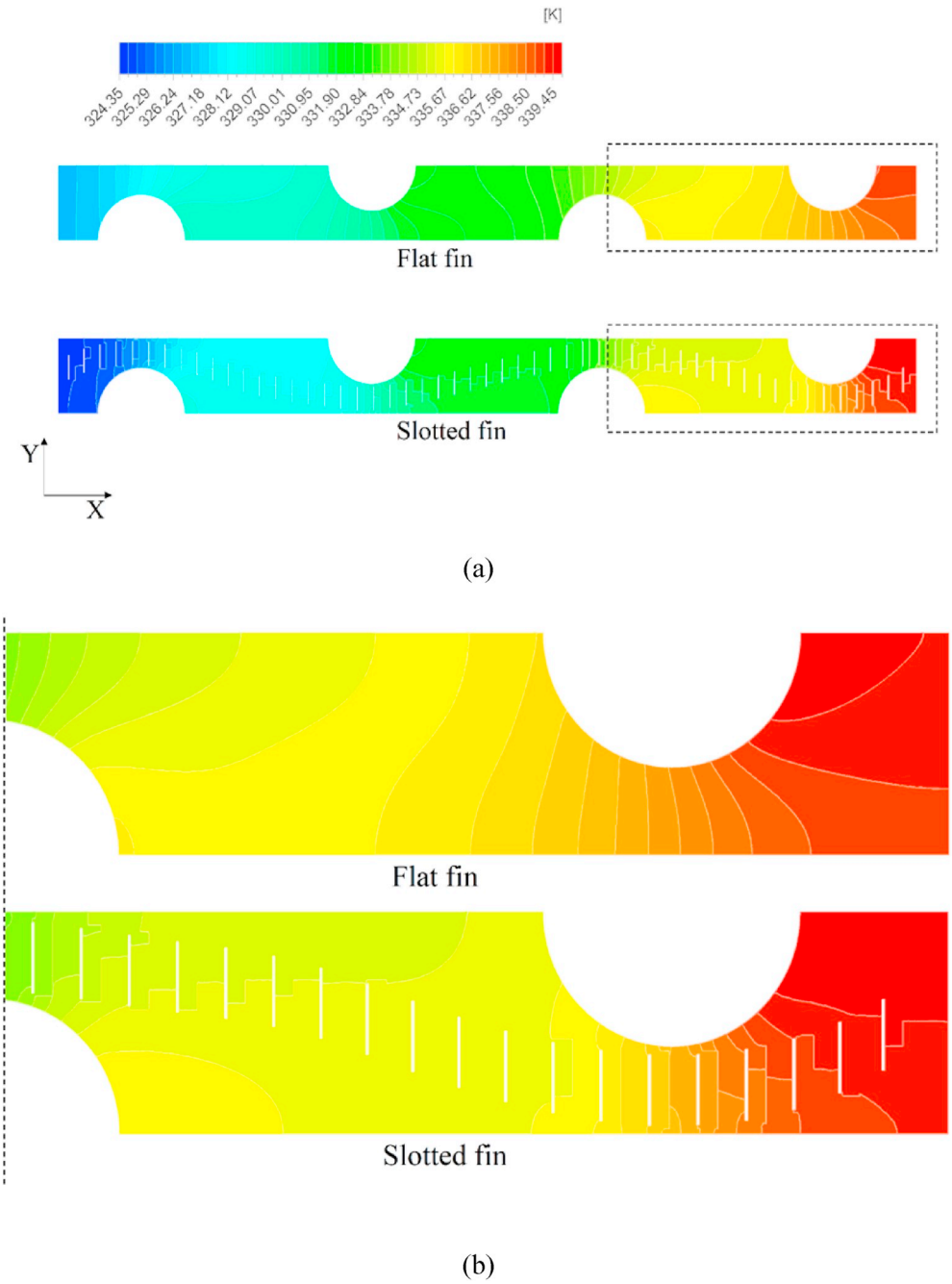

Fig. 7. Temperature distributions on the fin surface for slotted and flat fins (a) the whole fin surface (b) the enlarged view of the fin surface.

3. Results and discussion

3.1. The effects of the slot length and width on the overall performance

Fig. 7 compares the temperature on the fin surface for the flat fins and selected slotted fins (L = 2.1 mm and W = 0.5 mm), the enlarged views of the area enclosed by the dotted lines in Fig. 7(a) are shown in Fig. 7(b). It can be seen that on the most region of the slotted fin surface, the temperature is lower than that on the flat fin surface at the same location. And the high temperature region of the slotted fin surface is mainly concentrated on the end of the slotted fin surface, as shown in Fig. 7(b). This is because there is more heat on the fin surface taken away by the air, and the air temperature on the end of slotted fin surface is higher, so the temperature of the solid fin surface on the end is higher. Though there are small difference of the temperature on the fin surface, the temperature distributions on the fin surface are indeed changed, and the outlet temperature of the air is raised from 336.7 °C to 337.3 °C. So the slot can indeed improve the heat transfer performance, and the enhanced fin surface can disturb the fluid flow and prevent the development of the boundary layer, as discussed above. The velocity vector distribution of the flat fins and slotted fins are shown in Fig. 8, it can be found that there is large backflow region behind the tube wall of the flat fins, the flow and heat transfer performance in this area are very weak, and the heat transfer performance in the backflow region must be improved. The arrangements of slots can effectively reduce the back flow region, and the velocity distribution is uniform, and the flow field is more disordered, as shown in Fig. 8 (a). It is obviously that the velocity on the slotted fin surface is larger, the secondary flow is generated behind each slot, as shown in Fig. 8(b), the flow behind the slots is more disordered, so the impact of the fluid on the surface is stronger, the effect

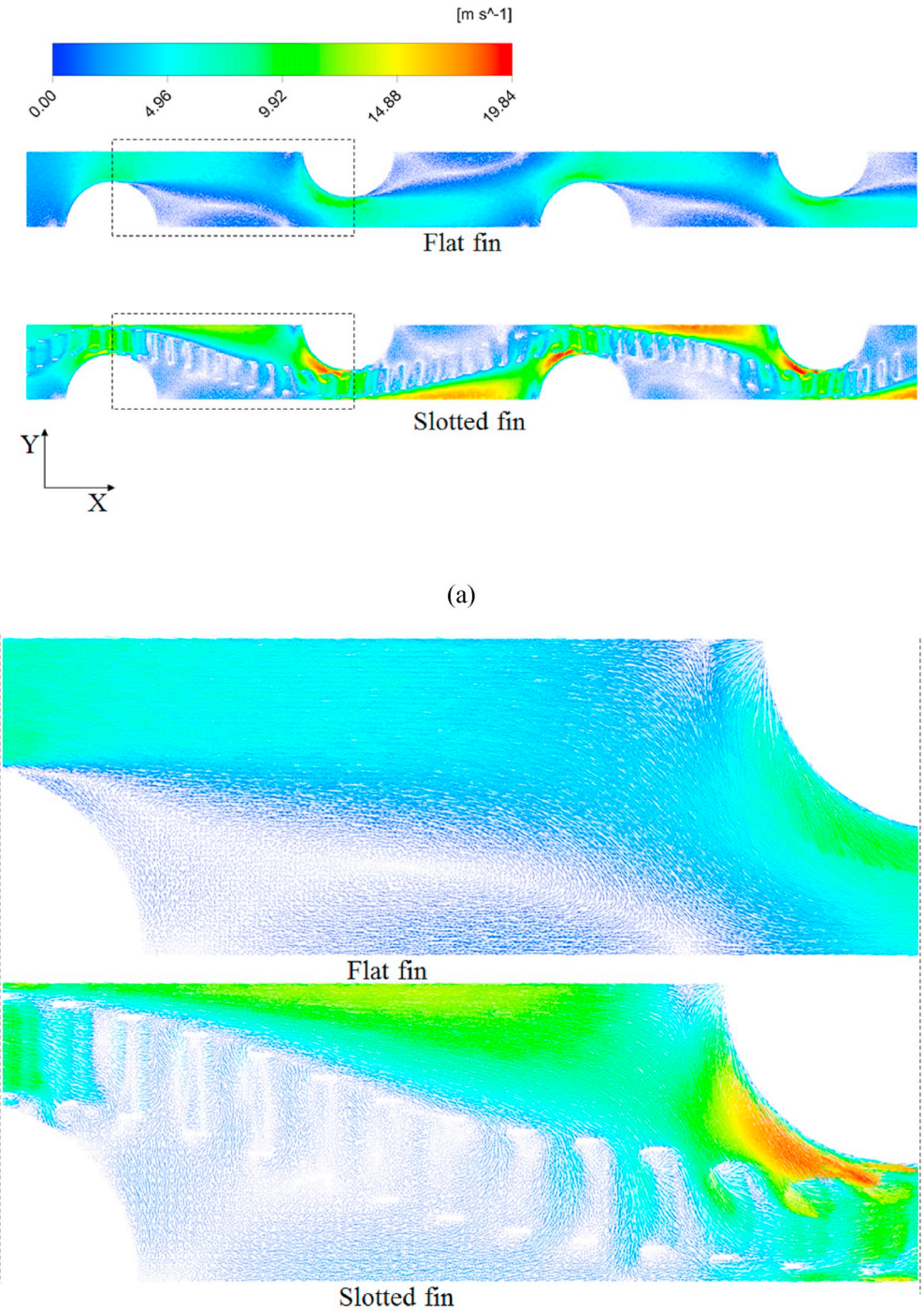

Fig. 8. Velocity vector distribution on the surface of slotted fin and flat fin (a) the whole fin surface (b) the enlarged view of the fin surface.

of convective heat transfer is better, and more heat flux is taken away, the performance of the heat transfer is enhanced. However, the large velocity and the disordered distribution of the velocity vector also leads to larger pressure drop, which means the improvement of heat transfer is at the cost of the power consuming, it is detrimental in engineering applications. Considering the combined effects of the heat transfer and the pressure drop, the overall performance of the slotted fins and the flat fins must be compared.

Figs. 9 and 10 represent the heat transfer and fluid flow performance, it is clearly that the heat transfer performance of all slotted fins is better than that of flat fins; while the flow performance of the slotted fins is worse than that of flat fins, the pressure drop is larger at the same *Re* number. As shown in Figs. 9(a) and 10(a), the *Nu* and friction factor vary in the same trend at different slot widths, *Nu* increases first and then decreases as the slot length increases, and the friction factor f increases linearly as the slot length increases. This is because when the slot length is short, the slot can well disturb the fluid flow, and destroy the boundary layer, which can effectively enhance heat transfer but cause a larger pressure drop. While with the further increase of the slot length, the slot is so long that leading to poor thermal conductivity of the metal

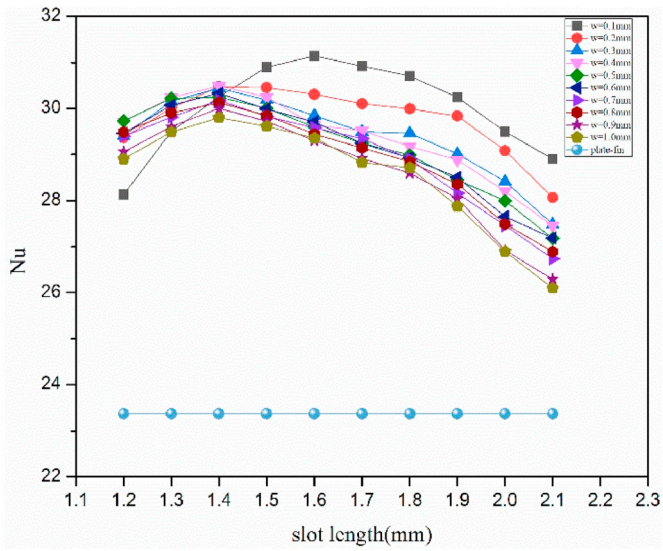

(a)

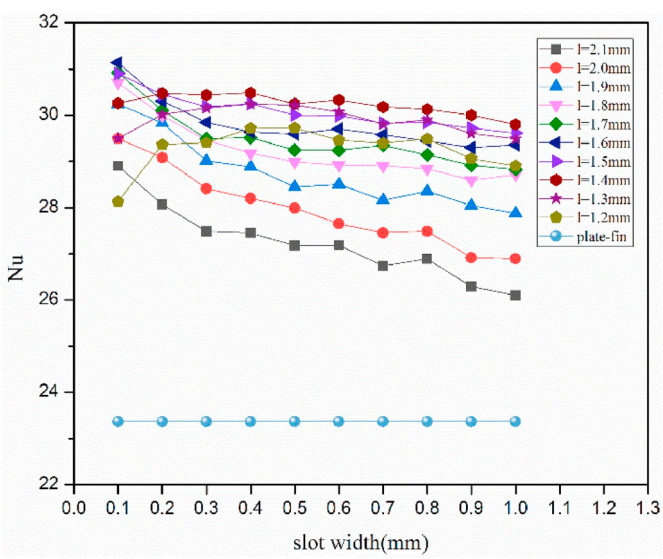

(b)

Fig. 9. (a) *Nu* varies with slot length (b) *Nu* varies with slot width.

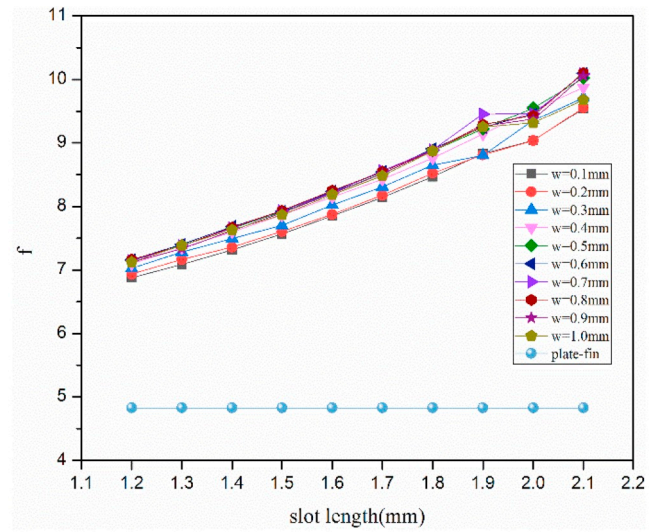

(a)

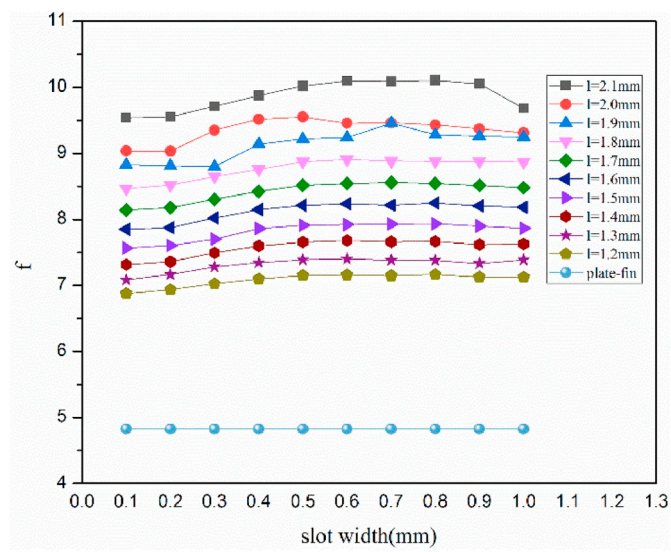

(b)

Fig. 10. (a) Friction factor varies with slot length (b) friction factor varies with slot width.

fins, so the heat transfer performance of the slotted find becomes poor; as for the friction factor, the longer slot length leads to smaller cross-section area, and the flow resistance as well as the pressure drop is greater, so the friction factor is larger. It can be seen from Fig. 9(b), when the slot length is shorter than 1.5 mm, *Nu* increases first and then decreases as the slot width increases; while when the slot length is between 1.5 mm and 2.1 mm, the *Nu* decreases as the slot width increases. This is because when slot length is shorter than 1.5 mm, the size of the slot is small, and the increase of the slot width can enhance the disturbance of fluid flow, reduce the thermal boundary layer and improve the heat transfer performance. Nevertheless, when the slot length is longer, the size of the slot is large and the increase of slot width leads to larger slot size, which causes poor thermal conductivity of the metal fins. The friction factor varies little with the increase of the slot width, as shown in Fig. 10(b), because the increases of slot width can slightly affect fluid flow.

Fig. 11 shows the overall performances of the slotted fins varying with the slot length and slot width, the performance of the flat fins is as the reference. Firstly, it can be found that the performance of some slotted fins is worse than that of the flat fins, while the performance of most slotted fins is better than that of the flat fins. The slots on the fin surface increase the heat transfer and the flow resistance at the same time, when the heat transfer enhancement is less than the cost of the increase of the flow resistance, the performance of the slotted fins is inferior to that of flat fins. Also it can be seen from Fig. 11 (a) that, for the different slot widths, the influence of the slot length on the overall performance is the same: with the increase of the slot lengths, the index j_C increases at first, and then decreases, moreover, with the further increase of the slot length, the j_C is lower than 1. While the influence of slot width on the overall performance depends on the slot length: when the slot length is small, with the increase of the widths, the index j_C increases first and then decreases; when the slot length increases, the increasing trend of the index j_C becomes weak, and when the slot length is larger than 1.5 mm, the index j_C decrease as the slot width W increases, as shown in Fig. 11 (b). So in the range of the parameters studied, there must exist a set of slot length and width to achieve the best overall

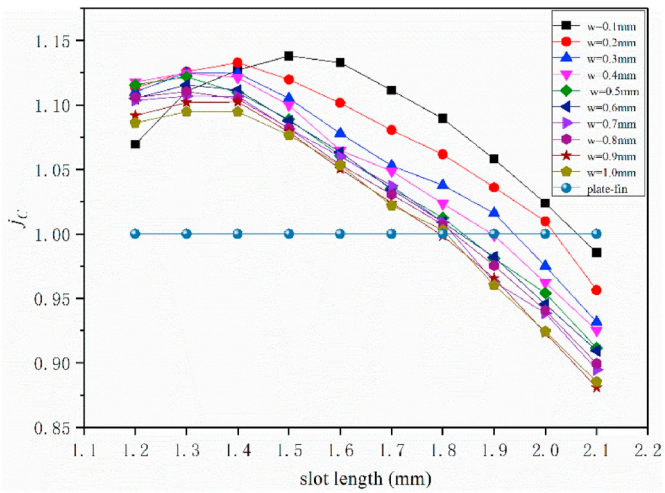

(a)

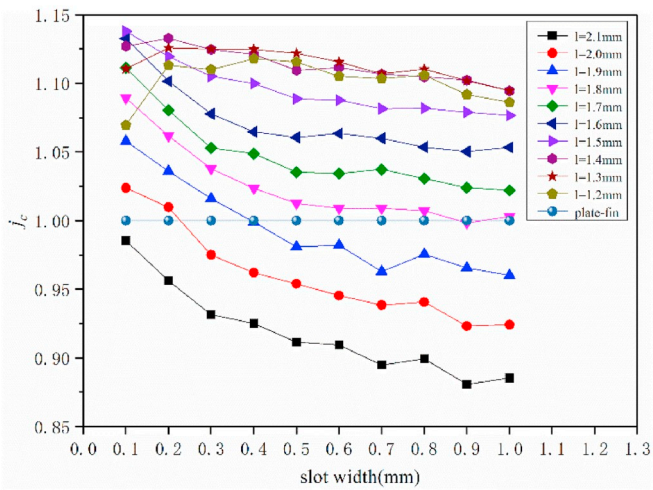

(b)

Fig. 11. (a) Overall performance at different slot lengths (b) Overall performance at different slot widths.

performance. Since the simulation error exists, some points on the graph fluctuate up and down, the graph is not very smooth, but the trend of all graphs is the same, so the above conclusion is reliable.

Based on the analysis above, the 100 sets of data of the overall performance is taken as the training database for the neural network, and the index j_C is adopted as the fitness for the GA to optimize and predict the results. The optimization tracing figure of GA based on the fitness j_C is shown in Fig. 12. It can be seen that after 37 generations, the average fitness consistent with the best fitness, the globally optimal parameters of slot length and width are solved, and the best fitness are achieved. The best overall performance given by the optimization is 1.131, and the slot length and width are L = 1.38 mm and W = 0.27 mm, respectively. This set of slot parameters is taken as the geometric parameters to build the physical model and the numerical simulation is carried out to verify the performance, the numerical result of the overall performance is 1.1268. The difference between the numerical result and the optimization result is less than 1%, so the accuracy of the optimization algorithm is believable and the parameters are recommended to get the best overall performance.

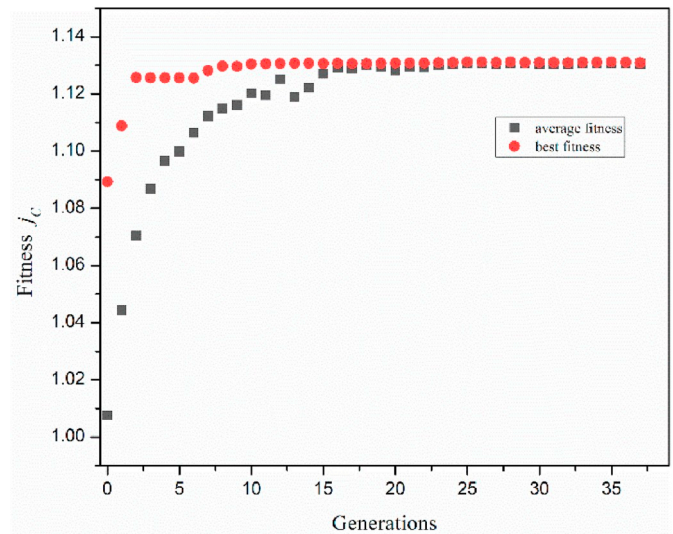

Fig. 12. The optimization tracing figures of GA based on fitness function j_C.

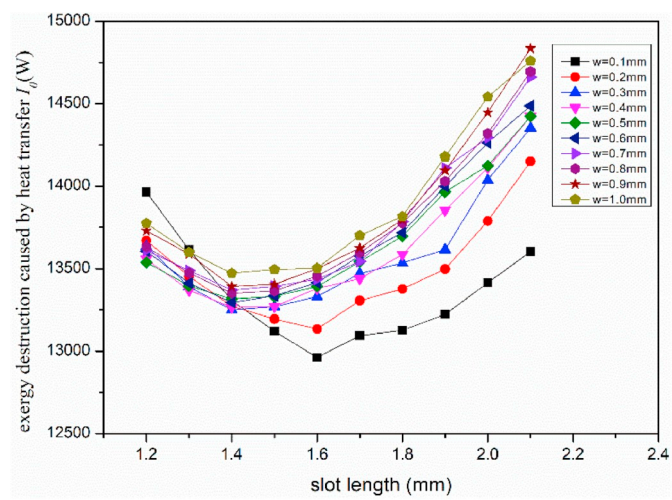

(a)

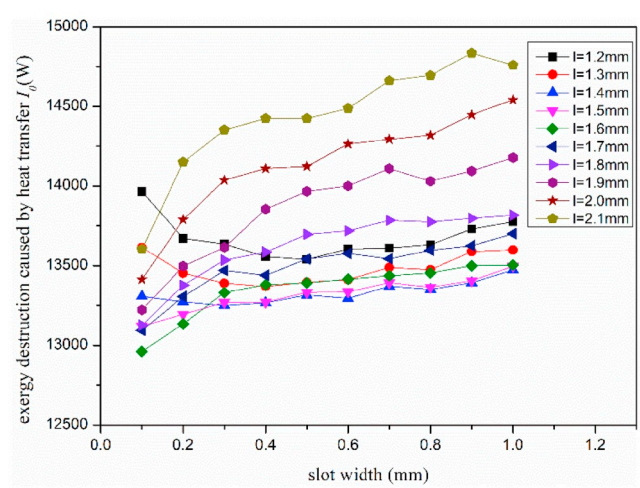

(b)

Fig. 13. The exergy destruction caused by the heat transfer (a) varies with the slot length (b) varies with the slot width.

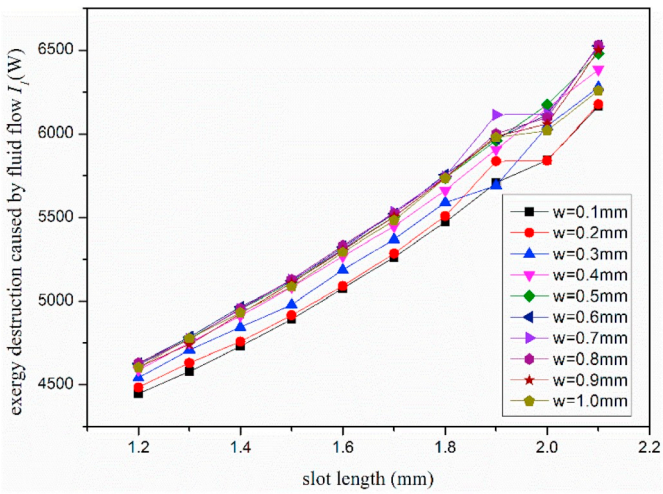

(a)

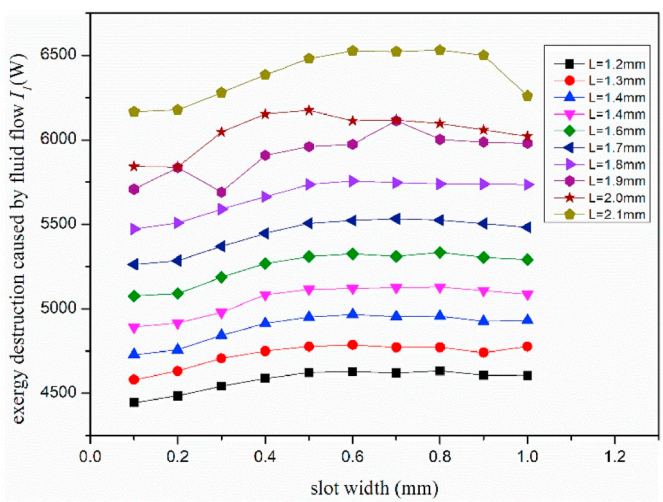

(b)

Fig. 14. The exergy destruction caused by the fluid flow (a) varies with the slot length (b) varies with the slot width.

3.2. The effects of the slot length and width on the exergy destruction

Fig. 13 and Fig. 14 represent the variation of the exergy destruction caused by the heat transfer and fluid flow. The exergy destruction caused by heat transfer represents the loss of the available energy. It can be found from Fig. 13 that with the increase of the slot length, the exergy destruction caused by transfer decreases first and then increases, and the smaller the slot width is, the more obvious this trend is, as shown in Fig. 13(a); while the variation of the heat transfer exergy destruction with the slot width depends on the length, when the slot length is small, the exergy destruction decreases first and then increases with the increase of the width, and when the slot length is greater than 1.5 mm, the exergy destruction decreases as the slot width increases, as shown in Fig. 13 (b). The variation of the exergy destruction with the slot parameters is related to the influence of the slot parameters on the temperature filed, namely, when the temperature gradient is decreased, the value of equation (11) is small and the exergy destruction is small. While the exergy destruction caused by the fluid flow totally represents the loss of the mechanical work, and it is directly related to the pressure drop. The exergy destruction caused by fluid flow is different from the exergy destruction caused by heat transfer, it increases almost linearly with the

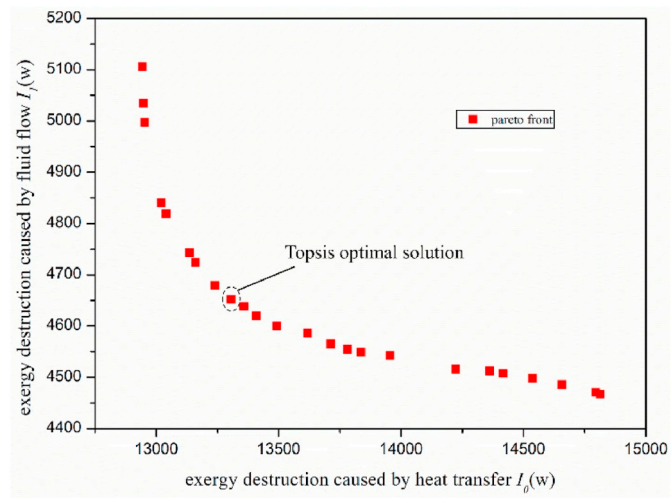

Fig. 15. Pareto front and Topsis optimal solution.

increase of the slot length, as shown in Fig. 14(a), while it increases slightly as the slot widths increase, as shown in Fig. 14 (b). This is because the increase of the slot length will reduce the flow cross-section area, which leads to the increase of the flow resistance, as a result, the loss of the mechanical work increases, and the exergy destruction increases as the slot length increases. And the increase of the slot width will increase the contact area between the fluids and solid, so the heat transfer performance and the mechanical work both increase, as shown in Figs. 13 (b) and 14 (b).

As discussed above, the exergy destruction represents the loss of available energy and mechanical work, so reducing the exergy destruction can improve the thermal quality of the gas, reduce the flow resistance and the power consumption [28]. On the one hand, in order to reduce the temperature gradient, obtain the uniform temperature field, it is necessary to minimize the exergy destruction caused by the heat transfer; on the other hand, the improvement of heat transfer inevitably leads to an increase in power consumption, in order to minimum the increase in power consumption and flow resistance, it is necessary to minimize the exergy destruction caused by the fluid flow, so I_0 and I_1 are chosen as the optimization objective. The ultimate purpose is to minimize the two exergy destruction, and the pareto front given by the optimization algorithm is shown in Fig. 15, a series of optimization solutions are given by the GA, and the best solution is found by The Topsis methods: the minimum exergy destruction caused by heat transfer is 13305.3 W, the minimum exergy destruction caused by fluid flow is 4652.142 W, as marked in Fig. 15, the corresponding slot length and width are 1.37 mm, 0.12 mm, respectively. This set of slot parameters is taken as the geometric parameters to build the physical model and the numerical simulation is carried out to verify the optimal results, the numerical results show that the I_0 and I_1 are 12948.7 W and 4595.9 W, respectively, the difference between them are under 2.69% and 1.21%, so the best solution is reliable and the slot parameters are recommended to obtain the minimum exergy destruction.

4. Conclusion

In this paper, the numerical simulation is carried out to study the influence of the slot parameters on the overall performance and the exergy destruction, the main findings are as follows:

1. The heat transfer performance of the slotted fins is better than that of the flat fins because of the enhanced surface geometry, while only the slotted fins with appropriate slot parameters have the better overall performance than the flat fins.

2. The effects of the slot length on the overall performance and the exergy destruction are great, while the effects of the slot width are slight. And there exist optimal solution of the overall performance and exergy destruction in the range of the slot parameters studied.
3. The overall performance is best when the slot length and width are 1.38 mm and 0.27 mm respectively, and the overall performance is 13.1% higher than that of flat fin.
4. The exergy destruction caused by heat transfer and fluid flow are minimized synergistically when the slot length and width are 1.37 mm and 0.12 mm, and the irreversible loss caused by heat transfer is reduced by 19.13% with the cost of an irreversibility increase of 40.6% caused by fluid flow
5. The difference between the two evaluation criteria proves that the best overall performance does not correspond to the minimum loss of the available energy and the mechanical work, which means the exergy destruction minimization also can be a principle to guide the heat transfer enhancement. The improvement of the thermal quality of the air in the outlet is significant and beneficial to improve the energy efficiency.

Declaration of competing interest

The authors claim that none of the material in the paper has been published or is under consideration for publication elsewhere.

Acknowledgment

The work is supported by State Key Laboratory of Air-conditioning Equipment and System Energy Conservation (No.ACSKL2018KT17) and the National Natural Science Foundation of China (NO. 51776079 & 51736004) and the National Key Research and Development Program of China (NO. 2017YFB0603501-3).

Appendix A. Supplementary data

Supplementary data to this article can be found online at https://doi.org/10.1016/j.ijthermalsci.2019.106133.

Nomenclature

A	Flow area (m^2)
A_c	Minimum flow area (m^2)
A_0	Total surface area (m^2)
C_p	Specific heat capacity of air (J/kg·K)
D	Diameter of the tube (mm)
D_h	hydraulic diameter (mm)
H	Height of the strips (mm)
L_{fin}	Length of the fin (mm)
L	Slot length (mm)
p	Pressure (Pa)
T	Fluid temperature (K)
$u_i u_k$	Velocity (m/s)
$u_{A\min}$	Velocity at the minimum flow area (m/s)
W	Slot width (mm)
S_t	Transverse tube pitch (mm)
S_l	Longitudinal tube pitch (mm)
δ	Fin thickness (mm)
ρ	Fluid density (kg/m^3)
Q	Total heat flux rate (W)
$\dot{m}$	Mass flow rate of air (kg/s)
μ	Dynamic viscosity (Pa·s)
λ	Thermal conductivity of air (W/m·K)
I_0	Exergy caused by heat transfer (W)
I_1	Exergy caused by fluid flow (W)
j_C	Index of overall performance
∇	Gradient

References

[1] M. Hatami, D.D. Ganji, M. Gorji-Bandpy, Numerical study of finned type heat exchangers for ICEs exhaust waste heat recovery, Case Stud. Therm. Eng. 4 (2014) 53–64.
[2] O. Pourmehran, M. Rahimi-Gorji, M. Gorji-Bandpy, M. Baou, Comparison between the volumetric flow rate and pressure distribution for different kinds of sliding thrust bearing, Propul. Power Res. 4 (2015) 84–90.
[3] S.E. Ghasemi, P. Valipour, M. Hatami, D.D. Ganji, Heat transfer study on solid and porous convective fins with temperature-dependent heat generation using efficient analytical method, J. Cent. South Univ. 21 (2014) 4592–4598.
[4] O. Pourmehran, M.M. Sarafraz, M. Rahimi-Gorji, D.D. Ganji, Rheological behaviour of various metal-based nano-fluids between rotating discs: a new insight, J. Taiwan Inst. Chem. Eng. 88 (2018) 37–48.
[5] Y.B. Tao, Y.L. He, J. Huang, Z.G. Wu, Numerical study of local heat transfer coefficient and fin efficiency of wavy fin-and-tube heat exchangers, Int. J. Therm. Sci. 46 (2007) 768–778.
[6] J.Y. Yun, K.S. Lee, Investigation of heat transfer characteristics on various kinds of fin-and-tube heat exchangers with interrupted surfaces, Heat Mass Transf. 42 (1999) 2375–2385.
[7] Naef A.A. Qasem, Abdulrahman A. Al-Ghamdi, Syed M. Zubair, An assessment of optimal airside heat transfer per unit friction power characteristics of compact heat exchangers, Int. J. Refrig. 99 (2019) 479–489.
[8] M. Hatami, D.D. Ganji, M. Gorji-Bandpy, Experimental and thermodynamical analyses of the diesel exhaust vortex generator heat exchanger for optimizing its operating condition, Appl. Therm. Eng. 75 (2014) 580–591.
[9] L. Gu, X. Ling, H. Peng, An experimental and numerical investigation of air side heat transfer and flow characteristics on finned plate configuration, Heat Mass Transf. 48 (2012) 1707–1721.

[10] H.J. Kang, W. Li, H.Z. Li, R.C. Xin, W.Q. Tao, Experimental study on heat transfer and pressure drop characteristics of four types of plate fin-and-tube heat exchanger surfaces, J. Therm. Sci. 3 (1994) 34–42.
[11] M. Bououd, A. Mechaqrane, K. Janusevicius, V. Martinaitis, Industrial solar drying System: modeling and design optimization of plate slotted fin-and-tube heat exchanger, Int. J. Renew. Energy Res. IJRER 9 (2019) 624–638.
[12] J.Y. Yun, K.S. Lee, Influence of design parameters on the heat transfer and flow friction characteristics of the heat exchanger with slit fins, Heat Mass Transf. 43 (2000) 2529–2539.
[13] Y.Q. Kong, L.J. Yang, X.Z. Du, Y.P. Yang, Air-side flow and heat transfer characteristics of flat and slotted finned tube bundles with various tube pitches, Int. J. Heat Mass Transf. 99 (2016) 357–371.
[14] L. Liu, X. Ling, H. Peng, Study on turbulent flow and heat transfer performance of tubes with internal fins in EGR cooler, Heat Mass Transf. 51 (2015) 1017–1027.
[15] G.N. Xie, Q.W. Wang, S. Bengt, Parametric study and multiple correlations on air-side heat transfer and friction characteristics of fin-and-tube heat exchangers with large number of large-diameter tube rows, Appl. Therm. Eng. 29 (2009) 1–16.
[16] Y.Q. Kong, L.J. Yang, X.Z. Du, Y.P. Yang, Effects of continuous and alternant rectangular slots on thermo-flow performances of plain finned tube bundles in in-line and staggered configurations, Int. J. Heat Mass Transf. 93 (2016) 97–107.
[17] H.Z. Li, H.J. Wang, M.Y. Yao, L.X. Zhang, H.F. Gu, J.P. Nie, PIV and thermal-vision experimental and numerical investigation on the airside performance of slotted fin surfaces, Int. J. Heat Mass Transf. 82 (2015) 568–580.
[18] X.Q. Wei, Y.H. Zhang, W.L. Hu, L.B. Wang, The fluid flow and heat transfer characteristics in the channel formed by flat tube and dimpled fin, Int. J. Therm. Sci. 104 (2016) 86–100.
[19] Z.Y. Guo, D.Y. li, B.X. Wang, A novel concept for convective heat transfer enhancement, Heat Mass Transf. 41 (1998) 221–225.
[20] S. Wang, Z.X. Li, Z.Y. Guo, Novel concept and devices of heat transfer augmentation, in: Proceeding of 11th International Conference of Heat Transfer, vol. 5, Taylor & Francis, London, 1998, pp. 405–408.
[21] W. Liu, P. Liu, Z.M. Dong, K. Yang, Z.C. Liu, A study on the multi-filed synergy principle of convective heat and mass transfer enhancement, Int. J. Heat Mass Transf. 134 (2019) 722–734.
[22] Y.L. He, W.Q. Tao, F.Q. Song, W. Zhang, Three dimensional numerical study of heat transfer characteristics of plain plate fin-and-tube heat exchangers from view point of field synergy principle, Heat Fluid Flow 26 (2005) 459–473.
[23] W.W. Jin, Y.L. He, Z.G. Qu, C.C. Zhang, W.Q. Tao, Optimum design of two-row slotted fin surface with X-shape strip arrangement positioned by "front coarse and rear dense" principle, Part II: results and discussion, Numer. Heat Transf., Part A: Applications 50 (8) (2006) 751–777.
[24] W.Q. Tao, W.W. Jin, Y.L. He, Z.G. Qu, C.C. Zhang, Optimum design of two-row slotted fin surface with X-shape strip arrangement positioned by "front coarse and rear dense" princple, Part I: physical/mathematical models and numerical methods, Numer. Heat Transf. Part A: Appl. 50 (8) (2006) 731–749.
[25] A. Bejan, Entropy generation minimization: the new thermodynamics of finite-size devices and finite-time process, J. Appl. Phys. 79 (1996) 1191–1218.
[26] S.B. Zhou, L.G. Chen, F.R. Sun, Constructal entropy generation minimization for heat and mass transfer in a solid-gas reactor based on triangular element, J. Appl. Phys. D Appl. Phys. 40 (2007) 2545–3550.
[27] Z.Y. Guo, H.Y. Zhu, X.G. Liang, Entransy-A physical quantity describing heat transfer ability, Int. J. Heat Mass Transf. 50 (2007) 2545–2556.
[28] W. Liu, P. Liu, J.B. Wang, N.B. Zheng, Z.C. Liu, Exergy destruction minimization: a principle to convective heat transfer enhancement, Int. J. Heat Mass Transf. 122 (2018) 11–21.
[29] J.B. Wang, W. Liu, Z.C. Liu, The application of exergy destruction minimization in convective heat transfer optimization, Appl. Therm. Eng. 88 (2015) 384–390.
[30] J. Wang, Z. Liu, W. Liu, Evaluation of convective heat transfer in a tube based on local exergy destruction rate, Sci. China Technol. Sci. 59 (2016) 1494–1506.
[31] O. Pourmehran, M. Rahimi-Gorji, M. Hatami, S.A.R. Sahebi, G. Domairry, Numerical optimization of microchannel heat sink (MCHS) performance cooled by KKL based nanofluids in saturated porous medium, J. Taiwan Inst. Chem. Eng. 55 (2015) 49–68.
[32] Mohammad Rahimi-Gorji, Tahereh B. Gorji, Mofid Gorji-Bandpy, Details of regional particle deposition and airflow structures in a realistic model of human tracheobronchial airways: two-phase flow simulation, Comput. Biol. Med. 74 (2016) 1–17.
[33] M. Hatami, Nanoparticles migration around the heated cylinder during the RSM optimization of a wavy-wall enclosure, Adv. Powder Technol. 28 (3) (2016) 890–899.
[34] I. Ozkol, G. Komurgoz, Determination of the optimum geometry of the heat exchanger body via a genetic algorithm, Numer. Heat Transf., Part A: Appl. 48 (2005) 283–296.
[35] A. Zendehboudi, X. Li, Desiccant-wheel optimization via response surface methodology and multi-objective genetic algorithm, Energy Convers. Manag. 174 (2018) 649–660.
[36] Y. Wang, Y.L. He, D.H. Mei, W.Q. Tao, Optimization design of slotted fin by Numerical simulation coupled with genetic algorithm, Appl. Energy 88 (2011) 4441–4450.
[37] H.N. Sun, Y. Ge, W. Liu, Z.C. Liu, Geometric optimization of two-stage thermoelectric generator using genetic algorithm and thermodynamic analysis, Energy 171 (2019) 37–48.
[38] Y. Ge, F. Shan, Z. Liu, W. Liu, Optimal structural design of a heat sink with laminar single-phase flow using computational fluid dynamics based multi-objective genetic algorithm, J. Heat Transf. 9 (2018) 13–18.
[39] Y. Ge, Z.C. Liu, H.N. Sun, W. Liu, Optimal design of a segmented thermoelectric generator based on three-dimensional numerical simulation and multi-objective genetic algorithm, Energy 147 (2018) 1060–1069.
[40] Y. Ge, S.C. Wang, Z.C. Liu, W. Liu, Optimal shape design of a minichannel heat sink applying multi-objective optimization algorithm and three-dimensional numerical method, Appl. Therm. Eng. 148 (2019) 120–128.
[41] J.Q. Li, L. Yu, Using BP Nerual networks for the simulation of energy consumption, in: IEEE International Conference on Systems, Man, and Cybernetics, 2014. October 5-8. USA: San Diego.
[42] M. Rahimi-Gorji, O. Pourmehran, M. Gorji-Bandpy, D.D. Ganji, An analytical investigation on unsteady motion of vertically falling spherical particles in non-Newtonian fluid by Collocation Method, Ain Shams Eng. J. 6 (2015) 531–540.
[43] M. Hatami, D.D. Ganji, M. Gorji-Bandpy, Experimental and numerical analysis of the optimized finned-tube heat exchanger for OM314 diesel exhaust exergy recovery, Energy Convers. Manag. 97 (2015) 26–41.
[44] S.F. Ding, C.Y. Su, J.Z. Yu, An optimizing BP neural network algorithm based on genetic algorithm, Artif. Intell. Rev. 36 (2011) 153–162.
[45] Iebeling Kaastra, Milton Boyd, Designing a neural network for forecasting financial and economic time series, Neurocomputing 10 (1996) 215–236.
[46] Kalyanmoy Deb, Samir Agrawal, Amrit Pratap, T. Meyarivan, A fast elitist non-dominated sorting genetic algorithm for multi-objective optimization: NSGA-II, in: M. Schoenauer, et al. (Eds.), Parallel Problem Solving from Nature PPSN VI. PPSN, vol. 1917, Springer, Berlin, Heidelberg, 2000. Lecture Notes in Computer Science.
[47] C.C. Wang, K.Y. Chi, C.J. Chang, Heat transfer and friction characteristics of plain fin-and-tube heat exchangers, part II: Correlation, Int. J. Heat Mass Transf. 43 (2000) 2693–2700.
[48] Y.P. Cheng, Z.G. Qu, W.Q. Tao, Y.L. He, Numerical design of efficient slotted fin surface based on the filed synergy principle, Numer. Heat Transf., Part A: Applications 45 (2004) 517–538.